Journal of Non-Crystalline Solids 576 (2022) 121222

Contents lists available at ScienceDirect

Journal of Non-Crystalline Solids

journal homepage: www.elsevier.com/locate/jnoncrysol

Tunable magnetocaloric effect in Gd-based metallic glasses microalloying elements with different magnetism

Lin Xue [a,*], Liliang Shao [b], Zhida Han [c], Qiang Luo [b], Haobo Wang [c], Juntao Huo [d], Zongzhen Li [e], Baosen Zhang [f], Jiangbo Cheng [a], Baolong Shen [b,*]

[a] College of Mechanics and Materials, Hohai University, Nanjing 211100, China
[b] School of Materials Science and Engineering, Jiangsu Key Laboratory for Advanced Metallic Materials, Southeast University, Nanjing 211189, China
[c] Jiangsu Laboratory of Advanced Functional Materials, Changshu Institute of Technology, Changshu 215500, China
[d] Key Laboratory of Magnetic Materials and Devices, Ningbo Institute of Materials Technology & Engineering, Chinese Academy of Sciences, Ningbo, 315201, China
[e] Jiangsu JITRI Advanced Energy Materials Research Institute Co., Ltd. Changzhou 213000, China
[f] School of Materials Science and Engineering, Nanjing Institute of Technology, Nanjing 211167, China

ARTICLE INFO

Keywords:
Metallic glass
Thermal stability
Magnetocaloric effect
Refrigeration capacity

ABSTRACT

In this work, the thermal properties, magnetic behavior and magnetocaloric effect of the $Gd_{55}Co_{17.5}Al_{24.5}M_3$ (M = Mn, Fe and Cu) metallic glasses with minor substitution of elements exhibiting varying magnetisms were investigated. The metallic glasses exhibited good glass-forming ability and underwent a second-order magnetic transition. As compared with the original composition, the Curie temperature was improved by microalloying the antiferromagnetic Mn, nonmagnetic Cu and ferromagnetic Fe. The magnetocaloric properties of the BMGs could be tuned by the microalloying elements with varying magnetisms. The competitive magnetic entropy change of 8.94 J $kg^{-1}K^{-1}$ and a large relative cooling power of 940 J kg^{-1} under a field change of 5 T were obtained for the Fe-substituted and Mn-substituted BMGs, respectively. A combination of the large refrigeration capacity and considerable magnetic entropy change makes the $Gd_{55}Co_{17.5}Al_{24.5}M_3$ (M = Mn, Fe and Cu) BMGs attractive refrigerant candidates for application in the active magnetic refrigerators.

1. Introduction

With the increasing demands with respect to the environmental friendless and energy efficiency, the magnetic refrigeration technology based on the magnetocaloric effect (MCE) has found extensive commercial applications in the refrigerators [1]. As the core of the magnetic refrigeration technology, developing refrigeration materials with large MCE, low cost and convenient manufacturing near room temperature, has attracted an extensive research interest. Till date, a series of magnetocaloric materials have been developed, which are classified into two categories based on the magnetic phase transition type: first-order magnetic transition (FOMT) and second-order magnetic transition (SOMT) materials [2]. The materials with FOMT exhibit magnetic and structural transitions and demonstrate a significant MCE at the Curie temperature (T_C) in a narrow temperature range, accompanied with undesirable thermal and magnetic hysteresis, such as Gd-Si-Ge, La-Fe-Si, Mn-Fe-P and FeRh crystals [3–6]. In contrast, the materials with SOMT demonstrate a moderate MCE in a wide temperature range, accompanied with a negligible hysteresis, such as pure Gd, Fe- and Gd-based metallic glasses [2, 7]. Due to the broad transition temperature range, the SOMT materials usually exhibit a large refrigeration capacity (RC) which is favorable for use in the Ericsson cycle magnetic refrigerators, thus, attracting a significant research attention.

Owning to the disordered atomic structure, the metallic glasses possess a range of advantageous mechanical and functional properties, such as high strength, superior corrosion resistance and excellent magnetic properties, thus, making them promising functional materials [8, 9]. Due to the specific 4*f* electronic structure, the rare earth-based metallic glasses exhibit typical MCE [10–13]. Among these, the Gd-based metallic glasses exhibit good thermal stability, comparable MCE and high T_C. Thus, these materials are considered as the promising refrigerant candidates near room temperature. As the properties and microstructure of the metallic glasses exhibit a high sensitivity to the constituents, a series of Gd-based metallic glasses have been investigated by modifying the compositions. It was found that the addition of the Mn element decreased the T_C of Fe-based amorphous alloys, while the

* Corresponding authors. Lin Xue and Baolong Shen.
E-mail addresses: lin.xue@hhu.edu.cn (L. Xue), blshen@seu.edu.cn (B. Shen).

https://doi.org/10.1016/j.jnoncrysol.2021.121222
Received 6 September 2021; Received in revised form 6 October 2021; Accepted 8 October 2021

converse was observed in the Gd-based amorphous alloys [14, 15]. The magnetocaloric properties of $Gd_{55}Co_{35}M_{10}$ (M = Mn, Fe and Ni) amorphous alloys were investigated with the addition of different transition elements, and the $Gd_{55}Co_{35}Fe_{10}$ alloy was observed to show a high T_C of 268 K and a broad magnetic entropy change (ΔS_M) peak of ~x223C 200 K [16]. The $Gd_{65}Mn_{35-x}Ge_x$ ribbons were fabricated in fully amorphous state by substituting Ge for Mn, and $-\Delta S_M$ was noted to be improved in the $Gd_{65}Mn_{25}Ge_{10}$ alloy [17]. The partial substitution of Fe for Co in the Gd-based amorphous alloys improved the T_C value of the alloy [18, 19]. The magnetic and magnetocaloric properties have been reported to vary with the M elements in the $Gd_{60}M_{30}In_{10}$ metallic glasses (M = Mn, Co, Ni, Cu) [20]. The literature studies indicate that the elements with differing in the magnetic character have distinctive effects on the MCE of the Gd-based metallic glasses. However, the mechanism is yet unclear. The magnetic behaviors including the MCE of the metallic glasses are sensitive to the magnetism of the components. Thus, clarifying the influence of the elements differing in magnetism on MCE as well as its origin is of high significance for developing the refrigerants with excellent MCE.

In our previous study, the $Gd_{55}Co_{17.5}Al_{27.5}$ bulk metallic glass (BMG) with large glass-forming ability and excellent MCE was synthesized [21]. However, it shows low T_C value of 95 K. Aiming to further enhance the T_C and MCE values of the metallic glass as well as study the effect of the elements with varying magnetism on MCE of the Gd-based metallic glasses, the substitution of ferromagnetic, antiferromagnetic and nonmagnetic elements was selected. Subsequently, the thermal properties, magnetic behavior and MCE of the $Gd_{55}Co_{17.5}Al_{24.5}M_3$ metallic glasses with M = Mn, Fe and Cu were systematically investigated. The tailorable MCE of BMGs containing the M elements with different magnetism has been discussed further.

2. Experimental

Master ingots with nominal compositions of $Gd_{55}Co_{22.5}Al_{24.5}M_3$ (M = Mn, Fe and Cu) were prepared by arc-melting a mixture of pure Gd, Co, Al, Mn, Fe and Cu with purities higher than 99.9 wt.% under a high purity argon atmosphere. For short, the GdMn3, GdFe3 and GdCu3 are used hereafter, which stand for $Gd_{55}Co_{22.5}Al_{24.5}M_3$ metallic glasses with M = Mn, Fe and Cu, respectively. Each ingot was melted for five times to ensure a chemical homogeneity. Then cylindric rod samples with diameters of 1.5 and 3 mm were prepared by copper mold suction casting method. The amorphous nature of the samples was certified by X-ray diffraction with Cu $K\alpha$ radiation (XRD, Bruker D8). Thermal analysis for the as-cast amorphous rods was carried out by a differential scanning calorimetry (DSC, NETZSCH 404 F3). The values of glass transition temperature (T_g) and primary crystallization temperature (T_x) were determined from the DSC traces with the accuracy of ±1 K. Active energies of glass transition and primary crystallization are calculated using Kissinger equation from the DSC curves measured at heating rates of 5 to 50 K/min. The linear thermal expansion curves were obtained by a thermomechanical analyzer (TMA, Netzsch TMA 402 F3) through dilatometric measurements. BMG samples with a diameter of 1.5 mm and a height of 3 mm were heated from room temperature to 903 K with a heating rate of 20 K/min under a constant applied force of 0.2 N. The kinetic viscosity (η) was then calculated as following [22]: $\eta = \frac{\sigma}{3\dot{\varepsilon}}$, where σ and $\dot{\varepsilon}$ are stress and strain rate, respectively. Temperature and field dependences of the magnetization curves for the BMGs were measured by a SQUID magnetometer (Quantum Design, MPMS). Field cooling magnetization (M_{FC}) of the samples was measured on the heating course after initial cooling from 300 to 2 K, under an applied magnetic field of 0.01 T through the whole process. On the other hand, the zero-field cooling magnetization (M_{ZFC}) was measured on the heating course under an applied magnetic field of 0.01 T after initial cooling the sample from 300 to 2 K with zero field. Isothermal magnetization (M-H) curves were measured with a varying magnetic field increasing from 0 to 5 T at temperatures ranging from 10 to 200 K.

3. Results and Discussion

In this study, with the addition of 3 at.% Mn, Fe and Cu, the developed $Gd_{55}Co_{22.5}Al_{24.5}M_3$ BMGs are observed to possess good glass-forming ability and can be easily fabricated in bulk. Fig. 1(a) shows the XRD patterns of the as-cast GdMn3, GdFe3 and GdCu3 rods with a diameter of 3 mm. The samples exhibit broad diffusion humps around 33° and 57°, with no sharp diffraction peak corresponding to crystalline phase, indicating the fully amorphous structure. The DSC curves of GdMn3, GdFe3 and GdCu3 BMGs with a heating rate of 20 K/min are displayed in Fig. 1(b). The glass transition process is noted to be followed by a wide supercooled liquid region, with sharp crystallization peaks, thus, further confirming the amorphous structure of the samples. As the substituted M element changes from Cu to Fe and Mn, the T_g value is observed to keep almost constant while the T_x value decreases, thereby resulting in a slight reduction in the supercooled liquid region. The detailed thermal parameters are listed in Table 1. All samples in this study exhibit a wide supercooled liquid region over 50 K, confirming their superior thermal stability.

To reveal the differences in the thermal stability and quantitatively analyze the changes in the T_g and T_x of the samples, the activation energies of glass transition and crystallization were calculated using the Kissinger equation [23]

$$\ln\frac{\varphi}{T^2} = -\frac{E_a}{RT} + \ln\frac{ZR}{E_a} \quad (1)$$

where φ is the heating rate, T is the specific temperature (T_g and T_x for the calculation here), R is the gas constant, E_a is the apparent activation

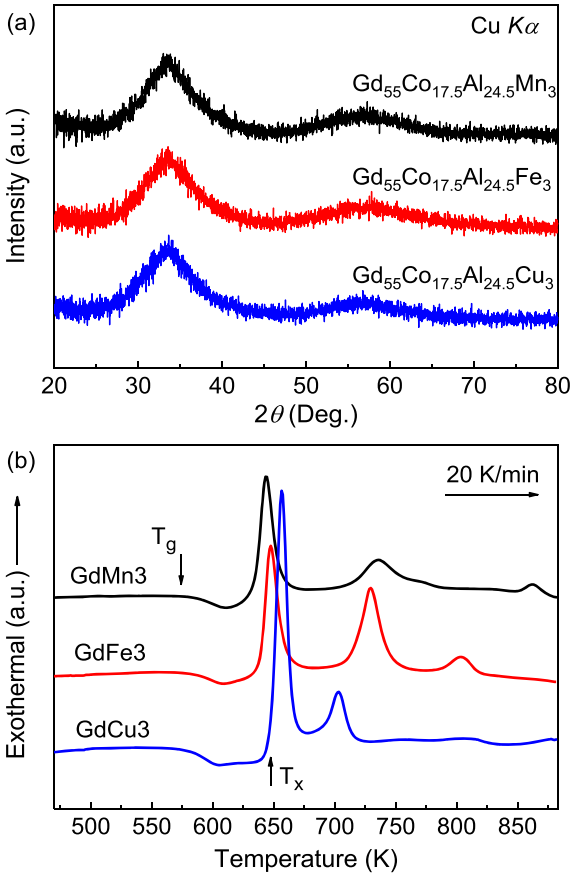

Fig. 1. (a) XRD patterns and (b) DSC curves of $Gd_{55}Co_{17.5}Al_{24.5}M_3$ (M = Mn, Fe and Cu) metallic glasses.

Table 1
Thermal parameters including T_g, T_x and ΔT_x, and magnetocaloric properties including T_C, $-\Delta S_M$ and *RCP* under a magnetic field change of 5 T of $Gd_{55}Co_{22.5}Al_{24.5}M_3$ (M = Mn, Fe and Cu) metallic glasses, as compared with some other Gd-based metallic glasses.

Composition	T_g /K	T_x /K	ΔT_x /K	T_C /K	$-\Delta S_M$ /J kg^{-1}K^{-1}	RCP /J kg^{-1}	Refs.
$Gd_{55}Co_{17.5}Al_{24.5}Mn_3$	584	635	51	114	8.56	940	This work
$Gd_{55}Co_{17.5}Al_{24.5}Fe_3$	582	639	57	118	8.94	918	This work
$Gd_{55}Co_{17.5}Al_{24.5}Cu_3$	580	648	68	100	8.0	740	This work
$Gd_{55}Co_{17.5}Al_{27.5}$	600	675	75	95	9.48	843	[21]
$Gd_{53}Al_{24}Co_{20}Zr_3$	599	653	54	93	9.4	590	[10]
$Gd_{0.6}Sc_{0.4})_{60}A1_{15}(Co_{0.6}Ni_{0.4})_{25}$	599	636	37	58	6.23	685	[12]
$(Gd_{0.667}Sc_{0.333})_{60}A1_{20}Co_{20}$	601	645	44	66	6.47	776	[12]
$Gd_{51}Al_{24}Co_{20}Zr_4Nb_1$	598	653	55	91	9.23	651	[10]
$Gd_{55}Co_{17}Al_{24}Si_1Fe_3$	598	666	68	117	7.83	838	[19]
$Gd_{55}Ni_{25}Al_{18}Zn_2$	552	591	39	84	9.33	849	[28]
$Gd_{51}Al_{24}Co_{20}Ce_5$	-	-	-	81	8.85	679	[10]
Gd (crystalline)	-	-	-	294	10.2	410*	[29]
$Gd_5Si_2Ge_2$ (crystalline)	-	-	-	276	18.4	360*	[29]

* The value was calculated by integration.

energy and Z is the frequency factor evaluating the number of collisions among the atoms participating in the crystallization reaction. The DSC curves for as-cast GdMn3, GdFe3 and GdCu3 BMGs were acquired at different heating rates, as shown in Fig. 2(a), (b) and (c). The experimental data could be fitted well by Eq. (1), as displayed in the insets. The activation energies of glass transition for GdMn3, GdFe3 and GdCu3 BMGs have been calculated to be 3.64, 4.05 and 4.18 eV, respectively, and the corresponding values of the primary crystallization are 2.40, 2.39 and 2.24 eV respectively. The activation energy of glass transition is observed to increase, while that of primary crystallization decreases gradually as M ranges from Mn to Fe and Cu. This indicates that the glass transition of the Cu- and Fe-substituted metallic glasses is more difficult than that of the Mn-substituted metallic glass, while the formation of the primary phase for these glasses is easily achieved. Furthermore, the viscosity of the GdMn3, GdFe3 and GdCu3 BMGs in the supercooled liquid region was measured, as shown in Fig. 2(d). For these three alloys, the discrete dots distribute around the onset temperature of glass transition, and the viscosity drops gradually with temperature, eventually increasing to the end temperature of glass transition. A significant decrease in the viscosity with the magnitude dropping from 10^{11} to 10^7 demonstrates the softening behavior of the metallic glasses in the supercooled liquid regions, where the atoms begin to rearrange and form clusters with different central atoms [24]. As the temperature increases above T_x, the viscosity is noted to increase promptly. It is noteworthy that the width of the supercooled liquid region characterized by a viscosity change is consistent with the DSC curves. Further, the GdMn3 BMG shows the smallest viscosity at T_x, thus, it has the lowest activation energy of primary crystallization.

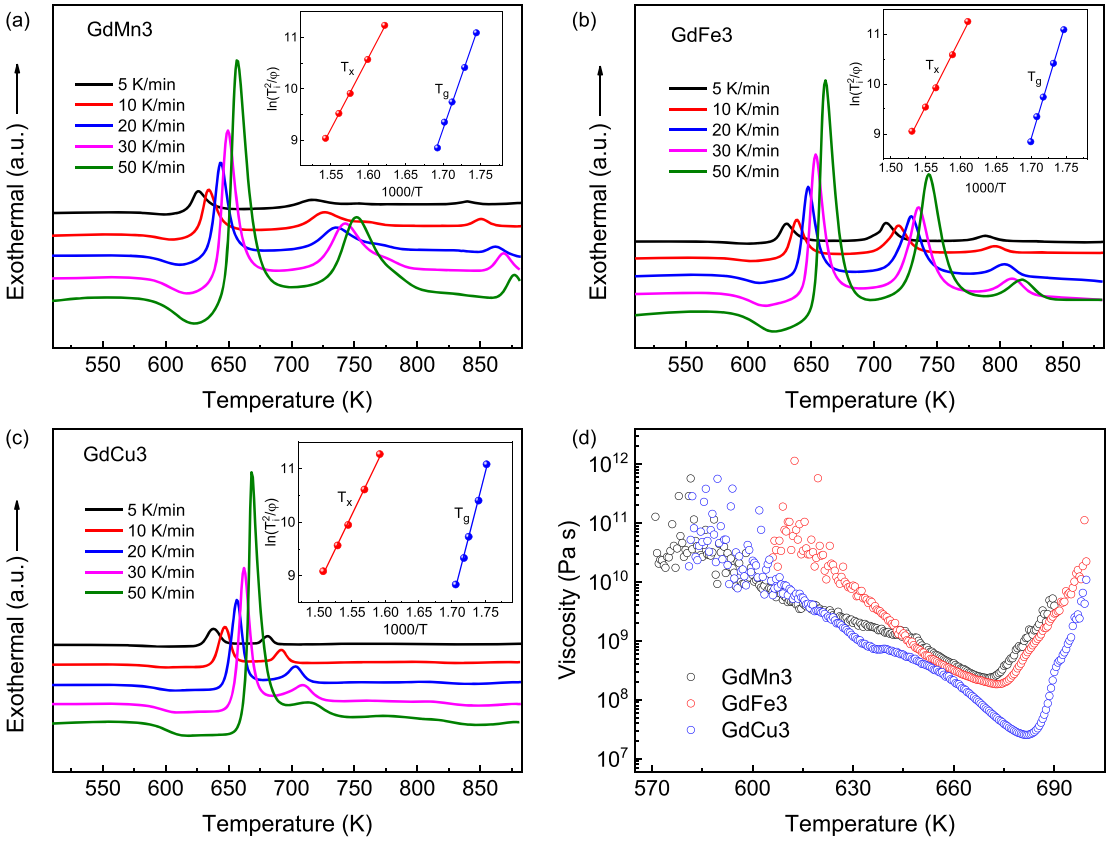

Fig. 2. DSC curves of $Gd_{55}Co_{17.5}Al_{24.5}M_3$ metallic glasses with M = (a) Mn, (b) Fe and (c) Cu at series heating rates. The insets present the Kissinger plots. (d) The viscosity of $Gd_{55}Co_{17.5}Al_{24.5}M_3$ (M = Mn, Fe and Cu) metallic glasses.

The temperature dependent magnetization (*M-T*) curves were measured to investigate the influence of minor addition of Mn, Fe and Cu on the magnetic behavior. Fig. 3 shows the *M-T* curves under an applied field of 0.01 T for the GdMn3, GdFe3 and GdCu3 glassy rods. The magnetic transition from ordering to disordering is noted to be accompanied with a pronounced decline in magnetization upon heating, thus, a magnetic transition from ferromagnetic to paramagnetic state is identified for the three samples. At low temperatures, the magnetization remains constant, which is affected by the demagnetization in the rod samples [19]. The T_C defined as the temperature corresponding to the minimum of the dM/dT curves is determined to be 114, 118 and 100 K for GdMn3, GdFe3 and GdCu3 BMGs, respectively, as marked in the inset of Fig. 3. The T_C value of the pristine $Gd_{55}Co_{17.5}Al_{27.5}$ BMG is 95 K [21], as listed in Table 1. A minor substitution of Mn, Fe and Cu for Al improves the T_C value of the alloy above 110 K, especially for the Fe-substituted BMG. This is comparable to 22 K rise with every 5 at.% Fe substitution with Co in the Gd-(Co, Fe) amorphous alloys [25]. According to the Rudermann-Kittel-Kasuya-Yosida (RKKY) indirect interaction theory, T_C shows a positive relationship with the indirect exchange interactions for the rare earth alloys as: $T_C = \frac{2}{3k_B} I(0)G$, where k_B is the Boltzman constant and $I(0)$ is the indirect exchange integral [26]. The exchange interactions depend locally on the interatomic distances in the rare elements and number of conduction electrons. In the $Gd_{55}Co_{17.5}Al_{27.5}$ metallic glass, the Co atoms exhibit a ferromagnetic coupling with Gd acting as the conduction electrons. The additional Mn, Fe, Cu atoms also act as the conduction electrons and promote the interactions among the Gd atoms in the alloys. Besides, the substitution of ferromagnetic Fe facilitates the magnetic coupling between Fe and Co, whereas that of antiferromagnetic Mn promotes the antiferromagnetic coupling between Mn and Co. The coefficient resulting in the enhancement of the indirect exchange integral thus improves the T_C value of BMGs. This indicates that a tunable T_C of BMGs can be designed by using the microalloying elements with varying magnetism.

To evaluate the magnetocaloric properties of the BMGs, the isothermal magnetization measurements ranging from 10 to 200 K were measured. Fig. 4 (a), (b), (c) present the isothermal magnetization curves (the insets) and corresponding Arrott plots for GdFe3, GdMn3 and GdCu3 BMGs, respectively. At temperatures below T_C, the samples are rapidly saturated under a small applied magnetic field. On increasing the temperature, both susceptibility and saturation magnetization are observed to decline, and a linear relationship between the magnetization and applied magnetic field can be observed at 200 K. It confirms a ferromagnetic transition of the samples, which is consistent

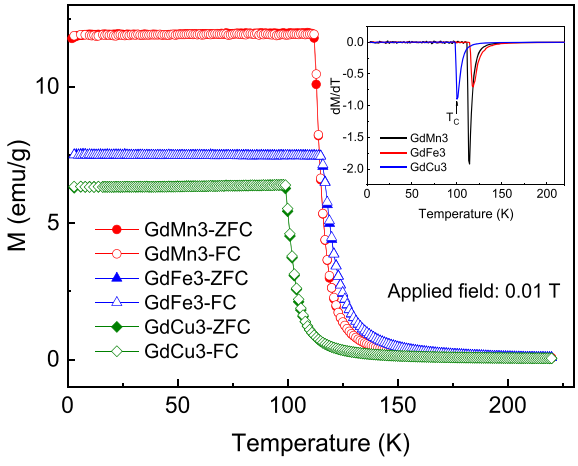

Fig. 3. Temperature dependence of zero field cooling (ZFC) and field cooling (FC) magnetization curves of $Gd_{55}Co_{17.5}Al_{24.5}M_3$ (M = Mn, Fe and Cu) metallic glasses under an applied field of 0.01 T. The inset shows the differential of the FC magnetization curves, and the Curie temperature is marked by arrows.

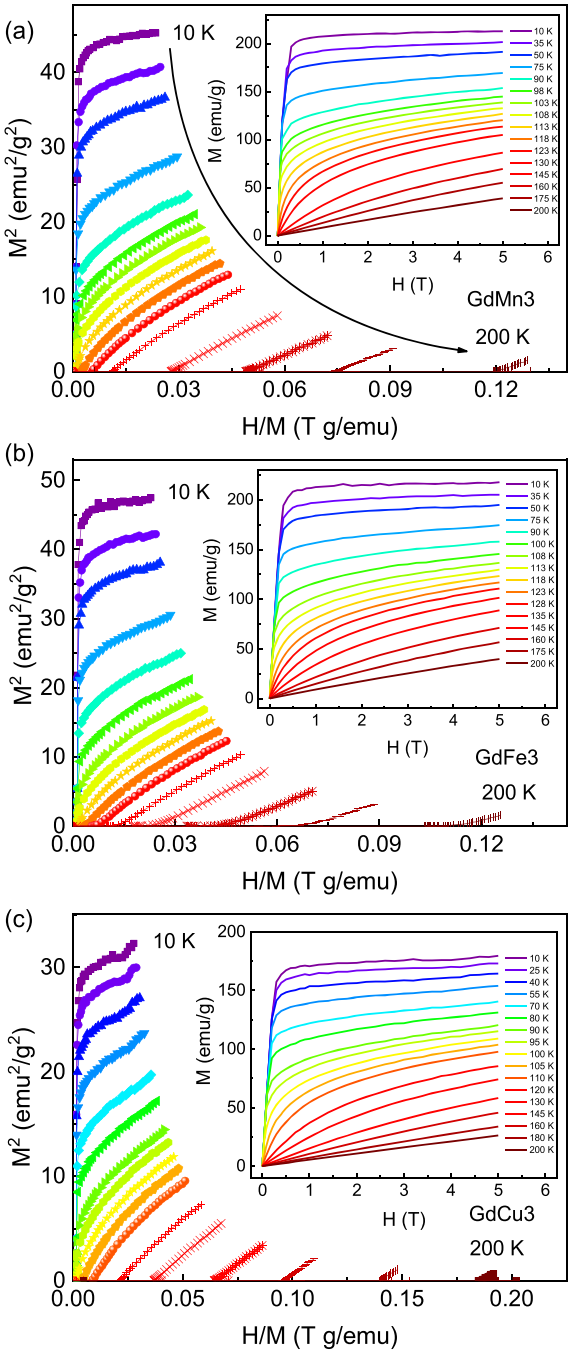

Fig. 4. Arrott plots of $Gd_{55}Co_{17.5}Al_{24.5}M_3$ metallic glasses with M = Mn (a), Fe (b) and Cu (c), respectively. The insets present the measured isothermal magnetization curves measured at temperatures from 10 to 200 K.

with the *M-T* curves shown in Fig. 3. According to the criterion proposed by Banerjee [27], the magnetic transition type can be determined by the Arrott plots, and the plots with negative slopes correspond to a FOMT, while the positive slopes represent a SOMT. The Arrott plots for GdMn3, GdFe3 and GdCu3 BMGs are presented in Fig. 4(a), (b) and (c), respectively. The Arrott plots are noted to exhibit positive slopes without inflection. Besides, the plots constitute a series of parallel straight lines around T_C and pass through the original point at T_C, thus, certifying that the samples experience a SOMT. Generally, the SOMT materials are more favorable for the active magnetic refrigerator applications, owing to the negligible loss and hysteresis. Fig. 5 shows the hysteresis loops of the samples, with the insets presenting the

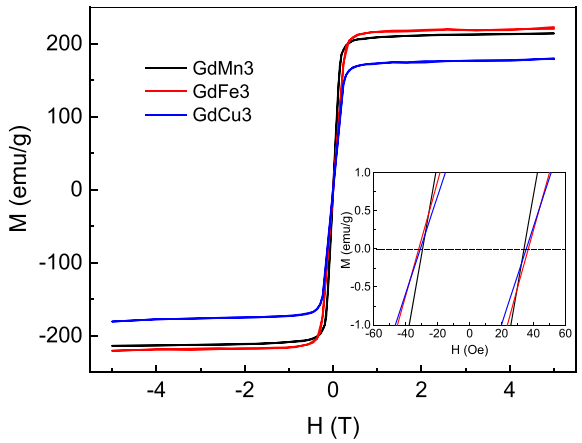

Fig. 5. Magnetic hysteresis loops of $Gd_{55}Co_{17.5}Al_{24.5}M_3$ (M = Mn, Fe and Cu) metallic glasses at 2 K. The inset shows the magnification.

amplification of the loops around zero magnetic field, As observed, the loops are coincident, and the samples reveal a small coercivity of about 0.003 T, thus, demonstrating a negligible hysteresis. Besides, it is noteworthy that the Cu-containing BMG shows a smaller magnetic susceptibility than those of the Mn and Fe-containing BMGs, along with the lowest saturation magnetization. The observed phenomenon is attributed to the dilution of the magnetic moment in the GdCu3 BMG caused by the introduction of the nonmagnetic Cu element. In contrast, owing to the ferromagnetic coupling between Fe and Co, the GdFe3 BMG reveals the largest saturation magnetization.

As one of the important parameters used to evaluate MCE of the magnetic refrigerants, the ΔS_M in this study was obtained by integrating the isothermal magnetization curves using the Maxwell relation [6]:

$$\Delta S_M(T,H) = S_M(T,H_2) - S_M(T,H_1) = \int_{H_1}^{H_2} \left(\frac{\partial M}{\partial T}\right)_H dH \quad (2)$$

where, H_2 and H_1 represent the maximum and minimum values of the applied magnetic field, respectively, and H_1 is set as 0 T in this study. Fig. 6(a), (b) and (c) present the temperature dependence of $-\Delta S_M$ for GdMn3, GdFe3 and GdCu3 BMGs under magnetic field varied from 0.5 to 5 T. The samples are noted to exhibit the same tendency, where $-\Delta S_M$ increases first, followed by a decrease as the temperature is increased, reaching a maximum in the vicinity of T_C. The peak values of the magnetic entropy change (ΔS_M^{pk}) for GdFe3, GdMn3 and GdCu3 BMGs at 5 T are determined to be 8.94, 8.56 and 8 J $kg^{-1}K^{-1}$, respectively. The obtained $-\Delta S_M^{pk}$ values are comparable to or even larger than those of the other Gd-based BMGs, as listed in Table 1. As observed from Table 1, the Gd-based metallic glasses exhibit good thermal stability, and various elements including Zr, Nb, Si, Fe, Zn and Ce have been substituted for improving the MCE of the Gd-based metallic glasses, however, most of these exhibit low T_C (below 100 K). With a minor addition of the Fe and Mn elements, the metallic glasses in this study exhibit the T_C values of 118 and 114 K, respectively, along with the comparable $-\Delta S_M$. It has been reported that a large value of the effective magnetic moment (μ_{eff}) in the Fe- and Tb-based metallic glasses corresponds to a more distinct magnetocaloric response [30, 31]. Accordingly, the μ_{eff} values for the GdFe3, GdMn3 and GdCu3 BMGs calculated from the M-T curves are determined to be 7.55, 6.76 and 6.14 μ_B, respectively. The values are noted to be consistent with the magnetisms of the corresponding

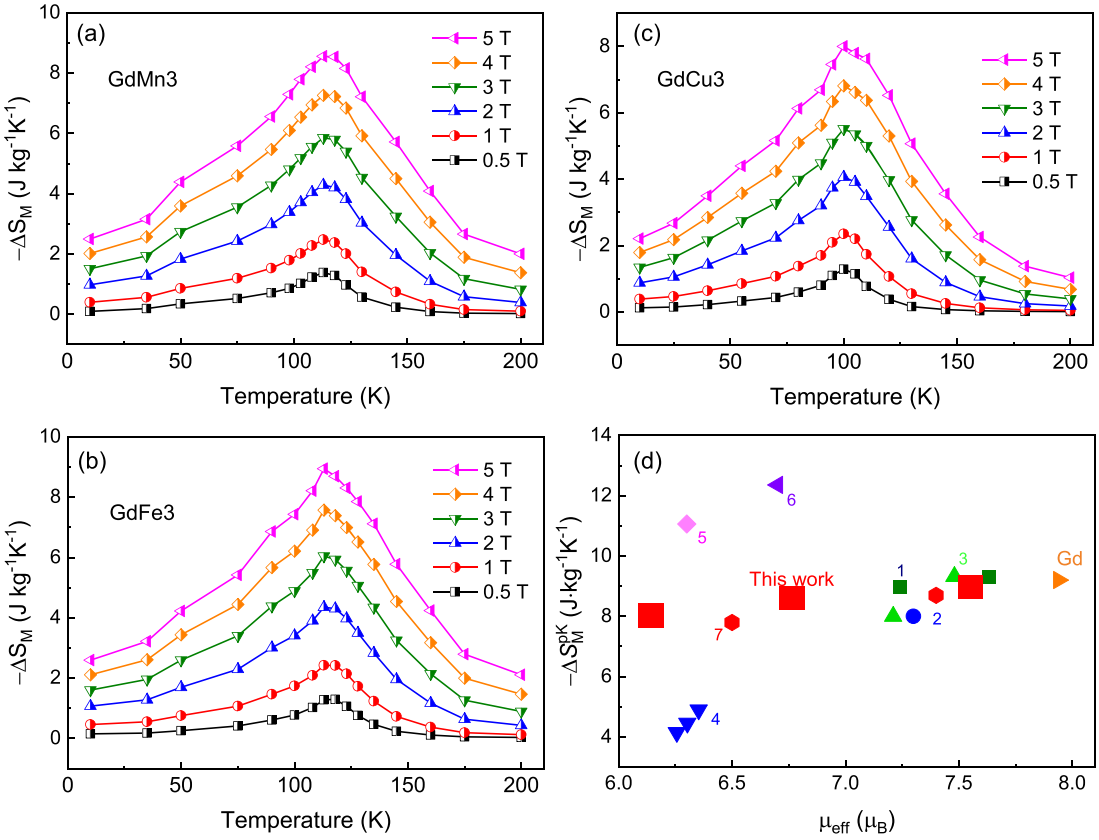

Fig. 6. (a), (b) and (c) The temperature dependence of $-\Delta S_M$ under different magnetic field change of $Gd_{55}Co_{17.5}Al_{24.5}M_3$ metallic glasses with M = Mn, Fe and Cu, respectively. (d) The peak value of $-\Delta S_M$ under a field of 5 T versus u_{eff} value of the Gd-based metallic glasses:1-$Gd_{55}Co_{25}Al_{20}$, $Gd_{55}Co_{25}Al_{18}Sn_2$ [32], 2-$Gd_{55}Al_{20}Ni_{12}Co_{10}Mn_3$ [33], 3-$Gd_{55}Al_{20}Ni_{20}Co_5$, $Gd_{55}Ni_{25}Al_{20}$ [34], 4-$Gd_{50}Co_{49}Ni_1$, $Gd_{50}Co_{48}Ni_2$ $Gd_{50}Co_{47}Ni_3$ [35], 5-$Gd_{34}Ni_{33}Al_{33}$ [36], 6-$Gd_{36}Tb_{20}Co_{20}Al_{24}$ [7], 7-$Gd_{55}Co_{19}Al_{24}Si_1Fe_1$ [19].

substituted elements as well as the $-\Delta S_M^{pk}$ values. Besides, the $-\Delta S_M^{pk}$ values under a magnetic field of 5 T versus the μ_{eff} values for a series of the Gd-based metallic glasses from Refs. [7, 19, 32–36] are presented in Fig. 6 (d). The $-\Delta S_M^{pk}$ values present a positive relationship with the u_{eff} values, but do not entirely depend on it. The metallic glasses in this study exhibit a relatively small μ_{eff} values, however, their $-\Delta S_M^{pk}$ values are comparable to most of the other Gd-based metallic glasses. As the $-\Delta S_M^{pk}$ value is affected by various factors, the $Gd_{34}Ni_{33}Al_{33}$ and $Gd_{36}Tb_{20}Co_{20}Al_{24}$ metallic glasses, fabricated into microwire shapes, also exhibit small μ_{eff} but large $-\Delta S_M^{pk}$ values [7, 36]. Nevertheless, the μ_{eff} values decrease as the Ni content increases in the $Gd_{50}Co_{50-x}Ni_x$ (x = 1, 2, 3) alloys, along with the $-\Delta S_M^{pk}$ values [35]. Thus, μ_{eff} can be used as a useful reference in the same alloy system.

For the SOMT material, a universal behavior of ΔS_M has been proposed by Franco *et al.*, which has been theoretically and experimentally confirmed near the magnetic transition temperature in the materials, including Gd metal, amorphous alloys and intermetallic species [37, 38]. The construction results in the normalized ΔS_M by ΔS_M^{pk} form as a function of the rescaled temperature can be expressed by the following description:

$$\theta = (T - T_C)/(T_r - T_C) \tag{3}$$

Where, T_r is the reference temperature, which was selected in correspondence to $|\Delta S_M|_{T_r} = 0.5\left|\Delta S_M^{pk}\right|$ above the T_C value in this study. As shown in Fig. 7(a-c), for each alloy, the normalized ΔS_M curves for different applied fields ranging from 0.5 to 5 T collapse to a universal curve. The observed uniformity further illustrates the single amorphous phase in the three metallic glasses with SOMT. Generally, the SOMT materials exhibit a broad temperature span of the magnetic transition, thus, leading to large *RC*, which is favorable for the practical applications.

RC presents the heat transferred between the hot and cold ends in an ideal refrigeration cycle. It was estimated by integrating the ΔS_M curve, i.e.,

$$RC = \int_{T_1}^{T_2} \Delta S_M dT \tag{4}$$

where, T_1 and T_2 present the low and high temperatures at the half maximum of $-\Delta S_M$, respectively [6]. Under a filed change of 5 T, the *RC* values are calculated to be 700, 676 and 550 J kg^{-1} for GdMn3, GdFe3 and GdCu3 BMGs, respectively. The *RC* values of the Mn- and Fe-containing metallic glasses are much larger than that of the $Gd_{20}Dy_{20}Er_{20}Ho_{20}Tb_{20}$ rare-earth high entropy alloy exhibiting giant MCE (about 627 J kg^{-1}) [39]. For materials with SOMT, the relative cooling power (*RCP*), defined as the product of $-\Delta S_M^{pk}$ and δT_{FWHM}, is commonly used, i.e.,

$$RCP = -\Delta S_M^{pk} \times \delta T_{FWHM} \tag{5}$$

where δT_{FWHM} is the full width at the half maximum of $-\Delta S_M$ [6]. For the studied BMGs, under a field of 5 T, the δT_{FWHM} values for GdMn3, GdFe3 and GdCu3 BMGs are determined to be 109.8, 102.7 and 92.5 K, whereas the *RCP* values are calculated to be 940, 918 and 740 J kg^{-1}, respectively. The *RC* and *RCP* values of the metallic glasses in this study are remarkably larger than those of the $Gd_5Si_2Ge_2$ and $Gd_5Si_2Ge_{1.9}Fe_{0.1}$ [40] crystalline materials as well as most of the reported Gd-based amorphous refrigerants. The high *RCP* values observed in this study can be attributed to the relatively large -ΔS_M value and broad δT_{FWHM}. The extension of δT_{FWHM} can be attributed to the gradual conversion of the magnetic moment in BMGs in the vicinity of T_C. The ferromagnetic coupling between Fe and Co and antiferromagnetic coupling between Mn and Co retard the magnetic phase transition, thus, leading to a wide transition temperature range over 110 K.

Both $-\Delta S_M^{pk}$ and *RCP* increase with the magnetic field and obey the exponential relationship: $|\Delta S_M| = AH^n$, $RCP = BH^N$, where *n* and *N* are the critical exponents, and *n* reflects the magnetic ordering state of the metallic glasses [41]. The $-\Delta S_M^{pk}$ and *RCP* values as a function of the applied magnetic field for the GdMn3, GdFe3 and GdCu3 BMGs are shown in Fig. 8(a) and (b), respectively. As observed, $-\Delta S_M^{pk}$ and *RCP* increase monotonously as the applied magnetic field is enhanced, and the data are fitted well by the exponential relationship (shown as the solid lines). The *n* values obtained for GdFe3, GdMn3 and GdCu3 BMGs are 0.81, 0.77 and 0.76, while *N* values are1.17, 1.13 and 1.16, respectively. The large values of *n* and *N* demonstrate a rapid increment in $-\Delta S_M$ and *RCP* on increasing the applied field. The *n* values are comparable to the other Gd-based and Fe-based metallic glasses, however, these slightly deviate from the theoretical value of 2/3 obtained from the mean field. The large *n* values in the amorphous alloys are generally attributed to the complex microstructure with the existence of the inhomogeneous structures like the chemical and atomic short-range order. Fig. 8(c) shows the plot of the *n* values versus temperature for the BMGs. The *n* value is closely related to the magnetic structure and magnetic transition in the alloys. It can be observed from Fig. 8(c) that the minimum value of *n* is located around T_C, and the *n* values tend to be 2 in the paramagnetic range due to the elimination of the short-range magnetic order. Below T_C, the *n* values increase due to the enhancement of the long-range magnetic order, whereas the values tend to be 1 at low temperatures in general. In this study, the values of *n* at low temperature are slightly larger than 1, as also observed in the original BMG and can be attributed to the existence of the magnetic clusters [21].

Fig. 9(a) displays the $-\Delta S_M^{pk}$, *RCP* and T_C values for GdMn3, GdFe3 and GdCu3 BMGs as compared with the $Gd_{55}Co_{17.5}Al_{27.5}$ metallic glass. With the minor substitution of the Mn and Fe elements, the magnetic exchange interaction of the alloy is noted to be enhanced, and the metallic glasses exhibit a distinct T_C improvement above 110 K. Especially, the T_C value of GdFe3 BMG is 118 K, which is 23 K larger than that of $Gd_{55}Co_{17.5}Al_{27.5}$. Despite a slight reduction in the $-\Delta S_M^{pk}$, the *RCP* values are also obviously improved by the substitution of Mn and Fe, with the values greater than 910 J kg^{-1}. For a more comprehensive comparison, the *RCP* and T_C data for various rare earth-based BMGs has been plotted in Fig. 9(b). As can be observed, the GdCo-based BMGs exhibit larger *RCP* with T_C values as compared with the DyCo-, HoCo-

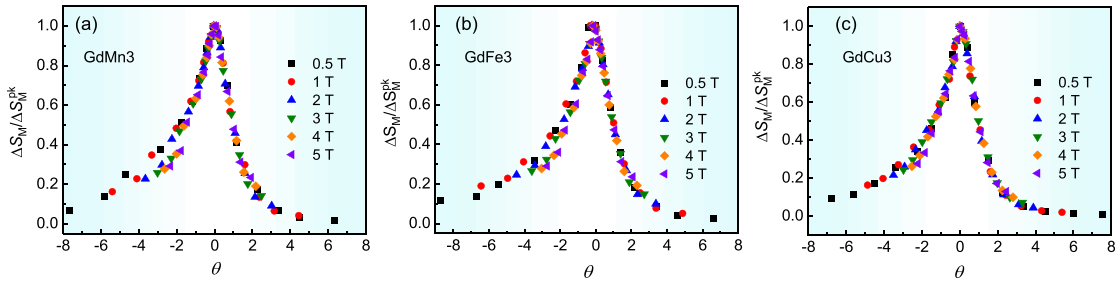

Fig. 7. (a), (b) and (c) Normalization of the ΔS_M for $Gd_{55}Co_{17.5}Al_{24.5}M_3$ metallic glasses with *M* = Mn, Fe and Cu, respectively.

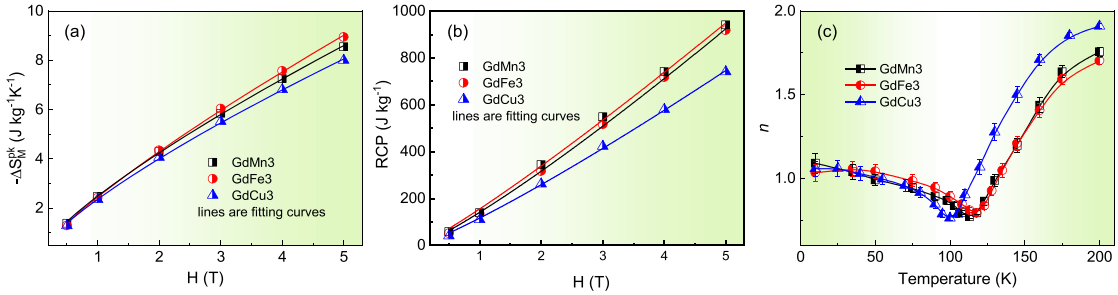

Fig. 8. (a) The peak value of $-\Delta S_M$ and *RCP* value (b) versus the applied field of $Gd_{55}Co_{17.5}Al_{24.5}M_3$ (M = Mn, Fe and Cu) metallic glasses. (c) Temperature dependent n values for the metallic glasses.

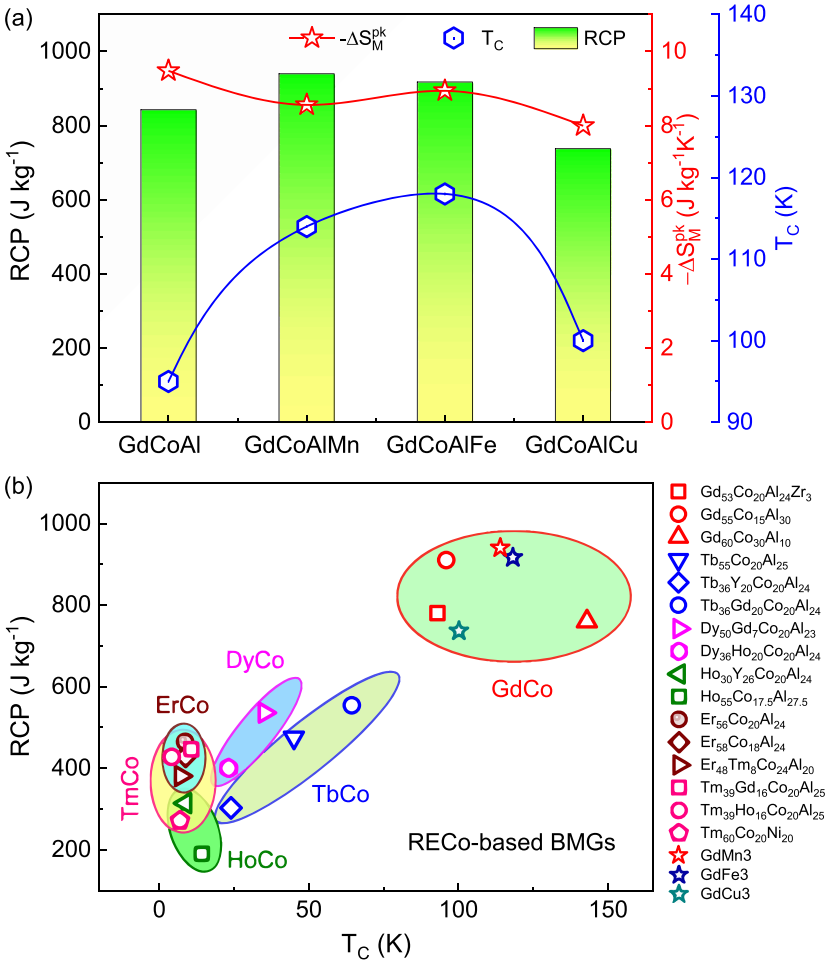

Fig. 9. (a) *RCP*, T_C and $-\Delta S_M$ values of $Gd_{55}Co_{17.5}Al_{24.5}M_3$ (M = Mn, Fe and Cu) metallic glasses. (b) The *RCP* versus T_C value for the metallic glasses in this study, as compared with various rare earth-based metallic glasses from Refs. [10, 42–51].

and ErCo-based metallic glasses [10, 42–51], thus, making them the favorable candidates for the refrigeration applications near room temperature. It is noteworthy that the *RCP* values of GdMn3 is 940 J kg^{-1}, which is noted to be the largest among the GdCo-based BMGs. In addition, as compared with the GdNi-based metallic glasses with significant *RCP* such as $Gd_{55}Ni_{30}Al_{15}$ (*RCP* of 851 J kg^{-1} and T_C of 83 K) [52], the *RCP* and T_C values of GdMn3 metallic glass are ~x223C 90 J kg^{-1} and 35 K larger, respectively. Therefore, the microalloying elements with an appropriate magnetism represent an effective method to prominently improve the *RCP* and T_C values of the Gd-based MGs without obvious decline in the ΔS_M values, which shed light on developing applicable magnetic refrigerants at room temperature.

4. Conclusion

In this study, the effect of the minor substitution of Mn, Fe and Cu with varying magnetism on the thermal stability, magnetic behavior and MCE of the Gd-based BMGs was investigated. With a minor M substitution, the indirect interactions are observed to be enhanced which improves the T_C values of the $Gd_{55}Co_{17.5}Al_{27.5}M_3$ (M = Mn, Fe and Cu) BMGs. Due to the ferromagnetic character of Fe with a large u_{eff} value, the Fe-substituted BMG exhibits a relatively large $-\Delta S_M$ value of 8.94 J kg^{-1}K^{-1}, under a magnetic field of 5 T. The wide transition temperature range and excellent *RCP* of 940 J kg^{-1} were obtained for the $Gd_{55}Co_{17.5}Al_{24.5}Mn_3$ BMG at 5 T, which is larger than most of the Gd-

based BMGs. In contrast, the addition of the nonmagnetic Cu element results in the dilution of the magnetic moment, leading to the low u_{eff}, magnetization, susceptibility and MCE in the Cu-contained BMG. Overall, the comparable ΔS_M and large *RCP* values combined with a negligible hysteresis make these Gd-based metallic glasses potential candidates for the refrigerant applications.

CRediT authorship contribution statement

Lin Xue: Methodology, Data curation, Investigation, Writing – original draft, Funding acquisition. **Liliang Shao:** Data curation, Investigation. **Zhida Han:** Writing – review & editing. **Qiang Luo:** Writing – review & editing. **Haobo Wang:** Investigation. **Juntao Huo:** Investigation. **Zongzhen Li:** Investigation. **Baosen Zhang:** Writing – review & editing. **Jiangbo Cheng:** Writing – review & editing, Funding acquisition. **Baolong Shen:** Conceptualization, Methodology, Project administration, Funding acquisition, Supervision, Writing – review & editing.

Declaration of Competing Interest

The authors declare that they have no known competing financial interests or personal relationships that could have appeared to influence the work reported in this paper.

Acknowledgements

This work was supported by the National Natural Science Foundation of China (Grant Nos. 52101193, 51631003 and 51975183), and Natural Science Foundation of Jiangsu Province, China (Grant No. BK20201316).

References

[1] A. Kitanovski, Energy Applications of Magnetocaloric Materials, Adv. Energy Mater. 10 (2020), 1903741.
[2] V. Franco, J.S. Blázquez, J.J. Ipus, J.Y. Law, L.M. Moreno-Ramírez, A. Conde, magnetocaloric effect: From materials research to refrigeration devices, Prog. Mater. Sci. 93 (2018) 112–232.
[3] J. Liu, C. He, M.X. Zhang, A.R. Yan, A systematic study of the microstructure, phase formation and magnetocaloric properties in off-stoichiometric La-Fe-Si alloys, Acta Mater. 118 (2016) 44–53.
[4] V. Chaudhary, X. Chen, R.V. Ramanujan, Iron and manganese based magnetocaloric materials for near room temperature thermal management, Prog. Mater. Sci. 100 (2019) 64–98.
[5] R.R. Gimaev, A.A. Vaulin, A.F. Gubkin, V.I. Zverev, Peculiarities of Magnetic and Magnetocaloric Properties of Fe-Rh Alloys in the Range of Antiferromagnet–Ferromagnet Transition, Phys. Metals Metallogr. 121 (2020) 823–850.
[6] K.A. Gschneidner Jr Jr, V.K. Pecharsky, Magnetocaloric materials, Ann. Rev. Mater. Sci. 30 (2000) 387–429.
[7] H.B.C. Yin, Y.J. Huang, Y. Bao, S.D. Jiang, P. Xue, S.S. Jiang, H. Wang, F.X. Qin, Z. Li, S.C. Sun, Y.F. Wang, H.X. Shen, J.F. Sun, Comparable magnetocaloric properties of melt-extracted $Gd_{36}Tb_{20}Co_{20}Al_{24}$ metallic glass microwires, J. Alloys Compd. 815 (2020), 150983.
[8] H.X. Li, Z.C. Lu, S.L. Wang, Y. Wu, Z.P. Lu, Fe-based bulk metallic glasses: Glass formation, fabrication, properties and applications, Prog. Mater. Sci. 103 (2019) 235–318.
[9] W.M. Yang, H.S. Liu, X.D. Fan, L. Xue, C.C. Dun, B.L. Shen, Enhanced glass forming ability of Fe-based amorphous alloys with minor Cu addition, J. Non-Cryst. Solids 419 (2015) 65–68.
[10] Q. Luo, W.H. Wang, Rare earth based bulk metallic glasses, J. Non-Cryst. Solids 355 (2009) 759–775.
[11] J.T. Huo, W. Sheng, J.Q. Wang, Magnetocaloric effects and magnetic regenerator performances in metallic glasses, Acta Phys. Sin. 66 (2017), 176409.
[12] S.A. Uporov, R.E. Ryltsev, V.A. Bykov, N.S. Uporova, S.Kh Estemirova, N. M. Chtchelkatchev, Glass-forming ability, structure and magnetocaloric effect in Gd-Sc-Co-Ni-Al bulk metallic glasses, J. Alloys Compd. 854 (2021), 157170.
[13] H.Y. Zhang, R. Li, L.L. Zhang, T. Zhang, Tunable magnetic and magnetocaloric properties in heavy rare-earth basedmetallic glasses through the substitution of similar elements, J. Appl. Phys. 115 (2014), 133903.
[14] Y.K. Fang, C.C. Yeh, C.C. Hsieh, C.W. Chang, H.W. Chang, W.C. Chang, X.M. Li, W. Li, Magnetocaloric effect in Fe-Zr-B-M (M = Mn, Cr, and Co) amorphous systems, J. Appl. Phys. 105 (2009) 07A910.
[15] Z.G. Zheng, X.C. Zhong, H.Y. Yu, V. Franco, Z.W. Liu, D.C. Zeng, The magnetocaloric effect and critical behavior in amorphous $Gd_{60}Co_{40-x}Mn_x$ alloys, J. Appl. Phys. 111 (2012) 07A922.
[16] X.C. Zhong, X.W. Huang, X.Y. Shen, H.Y. Mo, Z.W. Liu, Thermal stability, magnetic properties and large refrigerant capacity of ternary $Gd_{55}Co_{35}M_{10}$ (M = Mn, Fe and Ni) amorphous alloys, J. Alloys Compd. 682 (2016) 476–480.
[17] X.C. Zhong, J.X. Min, Z.G. Zheng, Z.W. Liu, D.C. Zeng, Critical behavior and magnetocaloric effect of $Gd_{65}Mn_{35-x}Ge_x$ (x = 0, 5, and 10) melt-spun ribbons, J. Appl. Phys. 112 (2012), 033903.
[18] B.Z. Tang, H.X. Xie, D.M. Li, L. Xia, P. Yu, Microstructure and its effect on magnetic and magnetocaloric properties of the $Co_{50}Gd_{50-x}Fe_x$ glassy ribbons, J. Non-Cryst. Solids 533 (2020), 119935.
[19] L. Xue, J. Li, W.M. Yang, C.C. Yuan, B.L. Shen, Effect of Fe substitution on magnetocaloric effects and glass-forming ability in Gd-based metallic glasses, Intermetallics 93 (2018) 67–71.
[20] C. Mayer, S. Gorsse, G. Ballon, R. Caballero-Flores, V. Franco, B. Chevalier, Tunable magnetocaloric effect in Gd-based glassy ribbons, J. Appl. Phys. 110 (2011), 053920.
[21] L.L. Shao, Q.Luo L.Xue, Q.Q. Wang, B.L. Shen, The role of Co/Al ratio in glass-forming GdCoAl magnetocaloric metallic glasses, Materialia 7 (2019), 100419.
[22] N. Nishiyama, A. Inoue, Glass transition behavior and viscous flow working of $Pd_{40}Cu_{30}Ni_{10}P_{20}$ amorphous alloy, Mater. Trans. Jim 40 (1999) 64–71.
[23] R.L. Blaine, H.E. Kissinger, Homer Kissinger and the Kissinger equation, Thermochim. Acta 540 (2012) 1–6.
[24] Z. Raza, B. Alling, I.A Abrikosov, Computer simulations of glasses: the potential energy landscape, J. Phys.: Condens. Matter. 27 (2015), 293201.
[25] Z.Y. Zhang, Q. Tang, F.C. Wang, H.Y. Zhang, Y.X. Zhou, A.L. Xia, H.L. Li, S.S. Chen, W.H. Li, Tailorable magnetocaloric effect by Fe substitution in Gd-(Co, Fe) amorphous alloy, Intermetallics 111 (2019), 106550.
[26] K.N.R. Taylor, M.I. Darby, Physics of Rare Earth Solids Chapman and Hall, 1972. London.
[27] S.K. Banerjee, On a generalised approach to 1st and 2nd order magnetic transitions, Phys. Lett. 12 (1964) 16–17.
[28] C. Wu, P. Yu, L. Xia, Glass forming ability and magnetic properties of a $Gd_{55}Ni_{25}Al_{18}Zn_2$ bulk metallic glass, J. Non-Cryst. Solids 422 (2015) 23–25.
[29] K.A. Gschneidner Jr, V.K. Pecharsky, A.O. Tsokol, Recent developments in magnetocaloric materials, Rep. Prog. Phys. 68 (2005) 1479–1539.
[30] Y.Y. Wang, X.F. Bi, The role of Zr and B in room temperature magnetic entropy change of FeZrB amorphous alloys, Appl. Phys. Lett. 95 (2009), 262501.
[31] Q. Luo, S. Bjoern, M. Norbert, E. Juergen, Giant irreversible positive to large reversible negative magnetic entropy change evolution in Tb-based bulk metallic glass, Phys. Rev. B 82 (2010), 024204.
[32] D. Ding, Y.Q. Zhang, L. Xia, Magneto-Caloric Response of a $Gd_{55}Co_{25}Al_{18}Sn_2$ Bulk Metallic Glass, Chin. Phys. Lett. 32 (2015), 106101.
[33] D. Ding, P. Wang, Q. Guan, M.B. Tang, L. Xia, Excellent Glass Forming Ability and Refrigeration Capacity of a $Gd_{55}Al_{20}Ni_{12}Co_{10}Mn_3$ Bulk Metallic Glass, Chin. Phys. Lett. 30 (2013), 096104.
[34] P. Wang, J.C. Chen, S. Lu, M.B. Tang, L. Xia, Effect of Minor Co Substitution for Ni on the Glass Forming Ability and Magnetic Properties of $Gd_{55}Ni_{25}Al_{20}$ Bulk Metallic Glass, Chin. Phys. Lett. 29 (2012), 096103.
[35] B.Z. Tang, X.P. Liu, D.M. Li, P. Yu, L. Xia, Effect of Ni substitution on the formability and magnetic properties of $Gd_{50}Co_{50}$ amorphous alloy, Chin. Phys. B 29 (2020), 056401.
[36] X. Wang, Q. Wang, B.Z. Tang, P. Yu, L. Xia, D. Ding, Large magnetic entropy change and adiabatic temperature rise of a ternary $Gd_{34}Ni_{33}Al_{33}$ metallic glass, J. Rare Earth. 39 (2021) 998–1002.
[37] V. Franco, A. Conde, Scaling laws for the magnetocaloric effect in second order phase transitions: From physics to applications for the characterization of materials, Int. J. Refrig. 33 (2010) 465–473.
[38] V. Franco, A. Conde, J.M. Romero-Enrique, J.S. Blázquez, A universal curve for the magnetocaloric effect: an analysis based on scaling relations, J. Phys.: Condens. Mat. 20 (2008), 285207.
[39] Y. Yuan, Y. Wu, X. Tong, H. Zhang, H. Wang, X.J. Liu, L. Ma, H.L. Suo, Z.P. Lu, Rare-earth high-entropy alloys with giant magnetocaloric effect, Acta Mater. 125 (2017) 481–489.
[40] V. Provenzano, A.J. Shapiro, R.D. Shull, Reduction of hysteresis losses in the magnetic refrigerant $Gd_5Ge_2Si_2$ by the addition of iron, Nature 429 (2004) 853–857.
[41] V. Franco, J.S. Blázquez, A. Conde, Field dependence of the magnetocaloric effect in materials with a second order phase transition: A master curve for the magnetic entropy change, Appl. Phys. Lett. 89 (2006), 222512.
[42] Y.K. Zhang, D. Guo, H.D. Li, S.H. Geng, J. Wang, X. Li, H. Xu, Z.M. Ren, G. Wilde, Low field induced large magnetic entropy change in the amorphousized $Tm_{60}Co_{20}Ni_{20}$ ribbon, J. Alloys Compd. 733 (2018) 40–44.
[43] X.H. Kou, Q. Luo, P.N. Dinh, J. Shen, Magnetocaloric response and its power law relationship with magnetoresistance in Er-Tm-Co-Al metallic glasses, J. Alloys Compd. 699 (2017) 591–595.
[44] J.T. Huo, D.Q. Zhao, H.Y. Bai, E. Axinte, W.H. Wang, Giant magnetocaloric effect in Tm-based bulk metallic glasses, J. Non-Cryst. Solids 359 (2013) 1–4.
[45] H. Zhang, R. Li, Y.F. Ji, F.M. Liu, Q. Luo, T. Zhang, Glass formation, magnetic properties and magnetocaloric effect of ternary Ho-Al-Co bulk metallic glass, J. Magn. Magn. Mater. 324 (2012) 4064–4067.
[46] X.D. Hui, Z.Y. Xu, Y. Wu, X.H. Chen, X.J. Liu, Z.P. Lu, Magnetocaloric effect in Er-Al-Co bulk metallic glasses, Sci. Bull. 56 (2011) 3978–3983.

[47] Q. Luo, B. Schwarz, N. Mattern, J. Eckert, Giant irreversible positive to large reversible negative magnetic entropy change evolution in Tb-based bulk metallic glass, Phys. Rev. B 82 (2010), 024204.
[48] J. Du, Q. Zheng, E. Bruck, K.H.J. Buschow, W.B. Cui, W.J. Feng, Z.D. Zhang, Spin-glass behavior and magnetocaloric effect in Tb-based bulk metallic glass, J. Magn. Magn. Mater. 321 (2009) 413–417.
[49] L. Liang, X.D. Hui, C.M. Zhang, G.L. Chen, A Dy-based bulk metallic glass with high thermal stability and excellent magnetocaloric properties, J. Alloys Compd. 463 (2008) 30–33.
[50] H. Fu, M.S. Guo, H.J. Yu, X.T. Zu, M. Liu, Amorphous composition in Gd–Co–Al system extracted from bulk metallic glass matrix composite, J. Appl. Phys. 106 (2009), 083513.
[51] B. Schwarz, N. Mattern, J.D. Moore, K.P. Skokov, O. Gutfleisch, J. Eckert, Influence of sample geometry on determination of magnetocaloric effect for $Gd_{60}Co_{30}Al_{10}$ glassy ribbons using direct and indirect methods, J. Magn. Magn. Mater. 323 (2011) 1782–1786.
[52] F. Yuan, J. Du, B.L. Shen, Controllable spin-glass behavior and large magnetocaloric effect in Gd-Ni-Al bulk metallic glasses, Appl. Phys. Lett. 101 (2012), 032405.